Performance of Fast Repetition Rate fluorometry based estimates of primary productivity in coastal waters

C. Robinson, D.J. Suggett, N. Cherukuru, P.J. Ralph, M.A. Doblin

PII: S0924-7963(14)00182-1
DOI: doi: 10.1016/j.jmarsys.2014.07.016
Reference: MARSYS 2593

To appear in: *Journal of Marine Systems*

Received date: 23 December 2013
Revised date: 12 May 2014
Accepted date: 10 July 2014

Please cite this article as: Robinson, C., Suggett, D.J., Cherukuru, N., Ralph, P.J., Doblin, M.A., Performance of Fast Repetition Rate fluorometry based estimates of primary productivity in coastal waters, *Journal of Marine Systems* (2014), doi: 10.1016/j.jmarsys.2014.07.016

Performance of Fast Repetition Rate fluorometry based estimates of primary productivity in coastal waters.

Robinson, C.[a, b], Suggett, D.J.[a], Cherukuru, N.[b], Ralph, P.J.[a], Doblin, M.A. [a*]

a. Plant Functional Biology and Climate Change Cluster, University of Technology Sydney, PO Box 123, Broadway, NSW 2007, Australia
b. CSIRO Land and Water, Black Mountain, GPO Box 1666, Canberra, ACT 2602, Australia

Keywords: estuary, coastal waters, phytoplankton, electron transport, ^{14}C, carbon fixation, primary production, light availability

Running title: FRRf estimates of coastal primary productivity

***** Corresponding author at: Plant Functional Biology and Climate Change Cluster, University of Technology Sydney, PO Box 123, Broadway, NSW 2007, Australia. Tel.: +61 2 9514 8307.

E-mail address: martina.doblin@uts.edu.au (M.A. Doblin).

Abstract

Capturing the variability of primary productivity in highly dynamic coastal ecosystems remains a major challenge to marine scientists. To test the suitability of Fast Repetition Rate fluorometry (FRRf) for rapid assessment of primary productivity in estuarine and coastal locations, we conducted a series of paired analyses estimating ^{14}C carbon fixation and primary productivity from electron transport rates with a Fast Repetition Rate fluorometer *MkII*, from waters on the Australian east coast. Samples were collected from two locations with contrasting optical properties and we compared the relative magnitude of photosynthetic traits, such as the maximum rate of photosynthesis (P_{max}), light utilization efficiency (α) and minimum saturating irradiance (E_K) estimated using both methods. In the case of FRRf, we applied recent algorithm developments that enabled electron transport rates to be determined free from the need for assumed constants, as in most previous studies. Differences in the concentration and relative proportion of optically active substances at the two locations were evident in the contrasting attenuation of PAR (400 – 700 nm), blue (431 nm), green (531 nm) and red (669 nm) wavelengths. FRRF-derived estimates of photosynthetic parameters were positively correlated with independent estimates of ^{14}C carbon fixation (P_{max} : n = 19, R^2 = 0.66; α : n = 21, R^2 = 0.77; E_K : n = 19, R^2 = 0.45; all $p < 0.05$), however primary productivity was frequently underestimated by the FRRf method. Up to 81% of the variation in the relationship between FRRf and ^{14}C estimates was explained by the presence of pico-cyanobacteria, chlorophyll-*a* biomass, and the proportion of photoprotective pigments, that appeared to be linked to turbidity. We discuss the potential importance of cyanobacteria in influencing the underestimations of FRRf productivity and steps to overcome this potential limitation.

1. Introduction

Primary production is a fundamental measure of an ecosystem's capacity to convert carbon dioxide into particulate organic carbon needed to fuel the foodweb, and thus underpins regulation of trophic dynamics and carbon cycling (Falkowski 2012). For decades, rates of marine primary productivity have been commonly measured using methods involving uptake of isotopically enriched inorganic carbon sources (Steeman-Nielsen 1952; Marra 2002; Kaiblinger & Dokulil 2006; Prieto et al. 2008; Lawrenz et al. 2013). Such methods have remained popular for a number of reasons, including their comparability with historic data. Additionally, the ^{14}C method is a sensitive technique which directly measures carbon assimilation that can be compared to standing stocks of organic carbon biomass. However, radioisotopes have become increasingly difficult to apply, largely due to greater health and safety regulations, and environmental restrictions limiting usage. This is of particular importance on small coastal vessels where the challenges of handling radioisotopes are greatest. This continues to present a major problem: the physical controls that underpin primary productivity in coastal waters are amongst some of the most dynamic over space and time, yet our understanding of how primary productivity varies in these waters remains largely unknown (Moore et al. 2003; Moore et al. 2006).

Active chlorophyll-*a* fluorometers have been designed to provide fast, non-invasive, accurate and accessible platforms to assess phytoplankton physiology and in turn determine photosynthetic rates (e.g. Kolber & Falkowski 1993; Suggett et al. 2011) and hence overcome many of the limitations associated with radioisotope-based measurements. For oceanographic studies, Fast Repetition Rate-based fluorometers (FRRfs) have been most commonly used to quantify photosynthetic rates, specifically the rate of electron transport through photosystem II (PSII), ETR_{PSII} (Kolber et al. 1998; Oxborough et al. 2012). In principal, ETR_{PSII}

measurements can be used to derive gross O_2 evolution or CO_2 uptake rates by applying a conversion factor that accounts for the various physiological pathways that effectively de-couple the ETR and O_2 evolution/CO_2 fixation from unity (Suggett et al. 2009a; Lawrenz et al. 2013); these non-linear processes include alternate electron sinks such as nitrate reduction (see Suggett et al. 2011). The factor accounting for the conversion from ETR_{PSII} to CO_2 uptake has recently been termed the electron yield [or requirement] for carbon fixation, $\Phi_{E:C}$ (Kromkamp et al. 2008, Lawrenz et al. 2013). Parallel measurements of ETR_{PSII} and O_2 production and/or CO_2 uptake can be correlated (Suggett et al. 2009a; Lawrenz et al. 2013) suggesting that single values of $\Phi_{E:C}$ can be applied. Notwithstanding, $\Phi_{E:C}$ values appear to be highly dependent upon the phytoplankton taxa and/or specific physical conditions of the marine environment (Lawrenz et al. 2013), and also potentially whether the phytoplankton are light-limited or light-saturated (Moore et al. 2006; Brading et al. 2013). Light-saturation requires that cells dissipate "excess" photochemical excitation pressure per unit of CO_2 fixed, therefore altering the conversion factor.

Methodological limitations associated with FRRF-based measures of ETR_{PSII}, as well as isotopically labelled carbon uptake, has been a major concern in reconciling the underlying factors that regulate $\Phi_{E:C}$ variability (Lawrenz et al. 2013). Most notably, ETR_{PSII} is determined by applying FRRf-derived parameters that quantify the light absorption (σ_{PSII}) as well as the quantum yield of photochemistry for PSII to a biophysical model which describes the absolute electron transport rate (Kolber & Falkowski 1993; Oxborough et al. 2012; see also Suggett et al. 2003). However, σ_{PSII} only describes the effective light absorption for PSII photochemistry relative to the number of active PSII "reaction centres" ([RCII]), i.e. those that can undergo photochemical charge separation, and thus [RCII] must be measured or assumed. Quantifying [RCII] is not straight-forward and only a handful of studies have

simultaneously measured both [RCII] and ETR_{PSII} on natural samples (Suggett et al. 2006; Moore et al. 2006; Oxborough et al. 2012). Other studies have typically assumed a constant value weighted by a photoinactivation factor, but this approach is flawed (see Suggett et al. 2004, 2011). Recently, Oxborough et al. (2012) developed a method to empirically determine [RCII] directly from FRRf photophysiological parameters; however, this approach has not yet been applied to determine how [RCII] varies in nature and the associated affect upon ETR_{PSII}, and in turn $\Phi_{E:C}$.

Here we apply new developments in FRRf-based ETR_{PSII} algorithms (Oxborough et al. 2012) to explore variability of $\Phi_{E:C}$ in coastal phytoplankton communities. Despite past efforts to examine $\Phi_{E:C}$, few studies have applied them to coastal waters (Smyth et al. 2004; Raateoja et al. 2004; Melrose et al. 2006; Moore et al. 2006; see also Napoléon and Claquin (2012) using Pulse Amplitude Modulation (PAM) fluorometry) and it is still unclear to what extent phytoplankton composition and/or environment plays in regulating $\Phi_{E:C}$ in such physically and bio-optically complex environments (Lawrenz et al. 2013). Our study focused on two locations with distinct bio-optical properties, a nearshore coastal time-series monitoring station and an urbanized estuary, with clear differences in physicochemical properties and water column structure (Pritchard et al. 2001, 2003; Lee et al. 2011). We expected that the bio-optical properties would be markedly different between sites, with greater light attenuation in the turbid estuary due to the presence of dissolved materials and non-algal particles which attenuate and filter light and thus influence the wavelengths and intensity of light for photosynthesis. We also predicted a strong relationship between FRRf and ^{14}C estimates of primary production. Additionally we expected that physical factors such as high light intensity and nutrient availability may result in some variability in the relationship between FRRf and ^{14}C based estimates of carbon fixation, and applied multivariate analyses

to identify key environmental and biological variables underlying the relationship between $\Phi_{E:C}$.

2. Methods

2.1. Water collection and measurement of environmental parameters

Phytoplankton assemblages were sampled from a historic time-series station at Port Hacking, NSW Australia (34°05'30'' S 151°15'30'' E) and in the Port Jackson Estuary (upper Parramatta River (33°49'462" S, 151°02'939" E) through to the lower estuary known as Sydney Harbour (33°51'001" S, 151°12 086" E) (Fig. 1). The coastal station (Port Hacking) is one of the longest biological time-series in the Southern Hemisphere (Thompson et al. 2009) and is located approximately 3 km offshore on the inner continental shelf. Here, water column stratification is seasonally dependent, where phytoplankton assemblages may be trapped in surface or sub-surface pycnoclines for days or weeks at a time (Pritchard et al. 2001). The Port Jackson estuary (approximately 30 km northwest of the coastal station) is a microtidal system, which is well mixed with semi-diurnal tides (Pritchard et al. 2003; Lee et al. 2011).

Maximum water depths at these sites were 100 m (Port Hacking, PH) and between 3 and 25 m (Sydney Harbour, SH). Water was collected at Port Hacking from the surface (3 m) and sub-surface fluorescence maximum (F_{max}; 35 – 45 m) during monthly intervals between May and August 2011, and in the Port Jackson estuary from 8 surface water (upper 1 m depth) stations in the same seasonal window during April and May 2011. Water was gently dispensed into 10 L polycarbonate bottles and stored in dim light (< 10 μmol photons m^{-2} s^{-1}) at ambient temperature until returning to the laboratory, approximately 4 hours after collection; these water samples were kept within 1-2 °C of ambient temperature during

transport and laboratory sampling. A CTD sensor (SBE 911plus, Sea-bird Electronics, Washington, USA) provided vertical profiles of temperature, salinity, chlorophyll-*a* fluorescence and CDOM fluorescence at each sampling station.

Downwelled irradiance was measured in the water column with a hyperspectral spectroradiometer (Ramses, Trios, Rastede, Germany) according to (Taylor et al. 2011) at 1 nm resolution between 344 and 750 nm. Photosynthetically active radiation (PAR 400 – 700 nm) was calculated using the following equation:

$$PAR = \int_{400\ nm}^{700\ nm} \mathrm{E}_d(\mathrm{z}) \quad (1)$$

The diffuse attenuation coefficient K_d (m^{-1}) for PAR (i.e. the mean across 400 – 700 nm) and at specific wavelengths (443, 531 and 669 nm) was calculated by linear regression of the natural logarithm of light irradiances versus depth (Stramski et al. 2008; Kirk 2011).

2.2. Phytoplankton pigments

Samples for photosynthetic and photoprotective pigment determination were filtered onto 25 mm glass fibre filters (Whatman GF/F, nominally 0.7 μm) and immediately frozen at -80 °C for later extraction in 90% acetone. Pigments were then analysed by high performance liquid chromatography (HPLC; Waters, Massachusetts, USA) using a C_8 column (Agilent Technologies, Victoria, Australia), following modified methods of Van Heukelem & Thomas (2001). Pigments were identified by their retention time and absorption spectrum; this method separates divinyl and monovinyl chlorophyll-*a*, zeaxanthin and lutein. Diagnostic pigment sums (Barlow et al. 2004) were applied to pigment concentrations to determine the proportion of photosynthetic (PSC; 19'-butanoyloxyfucoxanthin, diadinoxanthin, fucoxanthin, 19'-hexanoyloxyfucoxanthin, peridinin, violaxanthin) and photoprotective carotenoids (PPC; alloxanthin, β-carotene, diatoxanthin, lutein, zeaxanthin) in the total

pigment pool. Relative contribution of pigments to the total chlorophyll-*a* biomass were assigned to algal classes/groups using specific diagnostic pigments (Uitz et al. 2006; and applied to Australian waters by Thompson et al. 2011); specifically fucoxanthin, peridinin 19'-butanoloxyfucoxanthin, prasinoxanthin, 19'-hexanoloxyfucoxanthin, alloxanthin, zeaxanthin and divinyl chlorophyll-*a* as a proxy for the relative abundance of diatoms, dinoflagellates, pelagophytes, prasinophytes, coccolithophorids, cryptophytes, *Synnechococcus* sp., and *Prochlorococcus* sp., respectively, as well as neoxanthin, lutein and chlorophyll-*b* for chlorophytes.

2.3. Particulate absorption

Samples for phytoplankton light absorption analysis were collected to spectrally correct the productivity measurements (see below). Water samples were filtered onto 25 mm glass fibre filters (Whatman GF/F, nominally 0.7 µm) and preserved at -80°C for later analysis. Samples were analysed using the filter pad technique of Tassan & Ferrari (1995) and Mitchell et al. (2002). Samples from Port Hacking were analysed using a fibre optic UV/VIS spectrometer (Ocean Optics, Florida, USA). In this set-up, the light source supplied all wavelengths simultaneously with a measurement integration time of 4 ms and the sample blank was measured separately. Samples from Sydney Harbour were analysed on a dual beam UV/VIS spectrometer with integrating sphere (Perkin Elmer, Massachusetts, USA). In both analysis protocols, the sample path-length was accounted for, using the volume of water filtered onto the filter clearance area and the optical density of the filters, as per Tassan and Ferrari (1995). Absorption ($\alpha(\lambda)$) at wavelengths between 400 – 700 nm (units m^{-1}) was calculated using the following equation (Tassan & Ferrari 1995):

$$\alpha(\lambda) = 2.3\frac{A(\lambda)}{XC} \quad (2)$$

Where $A(\lambda)$ is the absorbance of the sample, corrected for optical density, X is the ratio of the volume of sample filtered (L) to the surface area of the filter clearance area (m^2), and C is the sample particle concentration (mass m^{-3}; assumed to be 1). Absorption at 1 nm intervals between 400-700 nm was normalized using HPLC-derived chlorophyll-*a* estimates to yield the chlorophyll-*a* specific absorption coefficient (denoted as $\alpha_{phy^*}(\lambda)$ with units m^2 (mg Chl-*a*) $^{-1}$).

2.4. FRRf measurements

Benchtop FRRf light-response measurements were based on routine protocols outlined previously (e.g. Suggett et al. 2003, 2009b, 2011). A *Fast*^{TRACKA} *MKII* FRRf housed within a *Fast*^{ACT} laboratory unit (Chelsea Technologies Group, UK) was programmed to deliver single turnover (ST) saturation of PSII induced by 100 flashlets of 1.1 μs at 2.8 μs intervals from an excitation source of blue LEDs (peak excitation 480 nm, see Fig. 2). All measurements were the average of 4 sequential ST measurements. Data was acquired every 40 seconds during exposure to 9 actinic light intensities (0, 5, 13, 21, 46, 71, 105, 181, 298 μmol photons m^{-2} s^{-1}) from a bank of white LEDs (calibrated by Chelsea Technologies Group with a 4π PAR quantum sensor, Walz GmbH, Germany) housed within the *Fast*^{ACT} (Fig. 2) Each actinic light intensity was applied for 4 minutes to ensure steady state fluorescence yields were consistently achieved (e.g. Suggett et al. 2003). Preliminary measurements on samples collected from both sites indicated that higher actinic intensities routinely induced low signal:noise such that variable fluorescence was negligible and photophysiological parameters could not be confidently derived; thus the actinic light intensity was kept below 300 μmol photons m^{-2} s^{-1}. In almost all cases, the FRRf-light response curves demonstrated that maximum, i.e. light-saturated, ETRs were achieved at light intensities well below 298 μmol photons m^{-2} s^{-1} (data not shown).

All FRRf acquisitions were fitted to the KPF model (Kolber et al. 1998) using *Fast*^{PRO} software to yield the key photophysiological traits; these included, minimum (F_0, F') and maximum (F_m, F_m') fluorescence yields, and PSII effective absorption (σ_{PSII}, $\sigma_{PSII'}$) for dark and actinic light conditions, respectively (Table 1) and non-photochemical quenching (NPQ = F_m/F_m' - 1). Additional variables calculated from the fluorescence yields were the PSII photochemical efficiency (F_v/F_m = [F_m-F_0]/F_m), and the fraction of [RCII] in the open state (1-*C*). Note that in past FRRf studies 1-*C* is estimated as q*P* (= (F'-F_0')/(F_m'-F_0') (Suggett et al. 2009a, Lawrenz et al. 2013), which reflects a "separate package model of connectivity" between RCIIs (see Oxborough et al. 2012). However, an alternative model q*J* (= (F'-F_0')/ (1- ρ) × (F_m'-F_0) + ρ × (F'-F_0) is used here where ρ is a parameter derived from the iterative curve fit of the fluorescence transient) of partial connectivity, which may be more representative of the dimer formation actually thought to occur in the photosynthetic apparatus (Oxborough et al. 2012). For our FRRf-light response data, estimates of q*P* and q*J* were generally the same for Port Hacking, whereas for Sydney Harbour estimates of q*J* were ~20-50% greater than those for q*P* (at intermediate actinic light intensities) (Fig. 2). The underlying nature of these differences is discussed later. All variables are dimensionless except for σ_{PSII}, which has units of nm^2 quanta^{-1}. Blanks of seawater filtered through 0.2 µm membrane filters (Millipore, Massachusetts, USA) were also analysed using identical protocols to determine whether dissolved optically-active constituents were contributing to the fluorescence signals. The baseline fluorescence (*F*) in the absence of cells was < 5% of the values from the unfiltered water samples, thus the background fluorescence was considered insignificant and therefore not removed from sample data.

2.5. Determination of FRRf-based CO_2 uptake rates

As with most previous studies (Lawrenz et al. 2013), the FRRf-based rate of gross photosynthesis (PC_{FRR}; mg C (mg Chl-*a*)$^{-1}$ h^{-1}) was calculated using the biophysical "sigma based" (sensu Oxborough et al. 2012) algorithm of Kolber and Falkowski (1993) following more recent modifications (Kaiblinger and Dokulil 2006; Suggett et al. 2009; Oxborough et al. 2012):

$$PC_{FRR} = E \times \sigma_{PSII'} \times (1/[F_v/F_m]) \times (1 - C) \times \frac{[RCII]}{(Chl{-}a)} \times \Phi_{E:C} \times 29.15 \quad (3)$$

where E is the irradiance (µmol photons m^{-2} s^{-1}), σ_{PSII} is the functional absorption cross section (nm^2 quanta^{-1}), C is the fraction of closed PSII reaction centres (1 - q*J*), [RCII] is the concentration of functional reaction centres (mol RCII m^{-3}), Chl-*a* is the concentration of monovinyl chlorophyll-*a* determined by HPLC and $\Phi_{E:C}$ is the electron requirement for carbon uptake (molecule CO_2 (mol electrons)$^{-1}$). The factor $(1/[F_v/F_m])$ accounts for non-radiative losses associated with σ_{PSII} (Suggett et al. 2009); See Table 1 for a list of the variable definitions. A conversion factor of 29.15 is applied in equation 3 to convert irradiance (E) from photons nm^2 s^{-1} to µmol photons m^2 h^{-1}, $\sigma_{PSII'}$ from nm^2 quanta^{-1} to m^2 mol [RCII]$^{-1}$, and electrons to carbon biomass per mg of chlorophyll-*a*. The ratio of electrons required for carbon fixation is assumed to be constant in this equation, i.e. photochemical charge separation yields 1 electron from 1 photon, and subsequently 4 moles of electrons are required to produce one molecule of O_2, which also fixes one molecule of carbon (Kaiblinger & Dokulil 2006). This assumption follows that any deviation from a one-to-one relationship for carbon fixation estimates yielded by the FRRf measurements and ^{14}C incorporation is due to variability in the electron to carbon ratio $(\Phi_{E:C})$. [RCII] (mol RCII m^{-3}) was determined following Oxborough et al. (2012) as,

$$[RCII] = \frac{K_R}{E_{LED}} \times \frac{F_0}{\sigma_{PSII}} \quad (4)$$

where K_R is an instrument specific constant (mol photons m^{-3} s^{-1}) and E_{LED} is the photon output from the FRRf measuring LEDs (photons m^{-2} s^{-1}). $\frac{K_R}{E_{LED}}$ (m^{-1}) was determined on another *Fast*^{TRACKA} *MKII* FRRf using phytoplankton cultures with a wide range of values of σ_{PSII} (*Dunaliella tertiolecta*, *Emiliania huxleyi*, *Ostreococcus* sp., *Pycnococcus provasolii*, *Synechococcus* sp., *Thalassiosira pseudonana*, *Thalassiosira weissfloggii*), from corresponding O_2-flash yield determinations of [RCII] and FRRf measures of F_0 and σ_{PSII} as per Oxborough et al. (2012; David Suggett & Antonietta Quigg, unpubl.). An additional FAST^{PRO} (v. 1.50.0.0) derived parameter, $[Chl]^{FRRf}$, automatically corrects for changes in the photomultiplier tube (PMT) sensitivity and LED excitation intensity (as calibrated against independent measures of a chlorophyll standard extracted in solvent) but also adjusts for any quenching of F_0 under actinic light. Thus, F_0 was substituted for $[Chl]^{FRRf}$ for the $\frac{K_R}{E_{LED}}$ determination. This $\frac{K_R}{E_{LED}}$ was subsequently corrected to account for differences in photon output between the instrument used to originally derive $\frac{K_R}{E_{LED}}$ and the instrument used in this study (following Oxborough et al. 2012) to yield a final value of 5.33 x 10^8 m^{-1}. [RCII] is thus calculated as the product of $\frac{K_R}{E_{LED}}$ and $\frac{[Chl]^{FRRf}}{\sigma_{PSII}}$. In the latter case, Eq. 3 can therefore be simplified to,

$$PC_{FRR} = E \times ([Chl]^{FRRf}/[F_v/F_m]) \times (\sigma_{PSII'}/\sigma_{PSII}) \times (1 - C) \times \frac{1}{(Chl-a)} \times \Phi_{E:C} \times 1.55 \times 10^{10} \quad (3)$$

where the conversion factor used in equation 3 has been further adjusted to account for the constant value for $\frac{K_R}{E_{LED}}$. It should be noted here that Oxborough et al. (2012) developed a modified approach to remove the need for (($\sigma_{PSII'}/\sigma_{PSII}$)x [RCII]) (= α_{LHII})) since measures of the effective absorption cross section can be unreliable at high light intensities. Here, (1-*C*) is replaced by with F_q'/F_m' (= $[F_m'-F']/F_m'$) and effectively eliminates the need to "choose"

a connectivity model; this method is termed the "absorption method" and basically substitutes $[(\sigma_{PSII'}/\sigma_{PSII}) \times [\text{[Chl]}^{\text{FRRf}}/[F_v/F_m] \times (1 - C)]$ for F_q'/F_m' in Eq 5. In order to contrast our data with past FRRf based studies, we continue to use the sigma-based method (Eq. 5), but return to differences with the absorption approach later in the discussion.

2.6. ^{14}C uptake

Short-term ^{14}C uptake incubations were performed using the small bottle method of Lewis & Smith (1983). For each station/depth, 162 mL of sample was inoculated with 6.327 x 10^6 Bq (0.171 mCi) $NaH^{14}CO_3$ and 7 ml aliquoted into 20 ml scintillation vials. Vials were placed on a custom made photosynthetron (halogen light source) for 1 h at 7 irradiances (0 – 2500 µmol photons m^{-2} s^{-1}). Light was passed through blue light filters (Ocean blue filter; LEE, California, USA) and light levels were measured before each day of use using a 4π quantum sensor (Li-cor, Nebraska, USA) immersed in water inside an incubation vial. Total initial activity was determined using 2 x 100 µL aliquots from an inoculated sample, with duplicate time zero samples used to correct for background counts. Following incubation, samples were acidified with 250 µL of 6 M HCl and degassed overnight in an orbital shaker. All samples were counted using a liquid scintillation counter (Perkin Elmer, Massashusetts, USA). Disintegrations per minute (DPM) were converted to units of carbon biomass (mg C) using the equation of Knap et al. (1996) and an estimate of the dissolved inorganic carbon for East Australian waters (2050 µmol L^{-1}; Hassler et al. 2011). The biomass values were normalized to chlorophyll-*a* concentration to yield PC_{14C} (mg C (mg Chl-*a*)$^{-1}$).

2.7. Comparison of FRRF and ^{14}C measurements

Spectral output of the light sources used by the photosynthetron, *Fast^{TRACKA} MKII*, and *Fast^{ACT}* were different (Fig. 2c); therefore FRRf-based spectrally-dependent parameters used

in the calculation of photosynthetic rates (and in turn used to derive P_{max}, α, and E_K) were corrected to equivalent values for the photosynthetron light source via calculations of the chlorophyll-*a* specific absorption coefficient weighted to each of the light spectra (termed $\bar{a}$) as per Moore et al. (2006), i.e. $\bar{a}^{TRON}$ (photosynthetron), $\bar{a}^{FT}$ (*Fast*^{TRACKA} *MKII*) and $\bar{a}^{FA}$ (*Fast*^{ACT}). Values for σ_{PSII} were adjusted as $\sigma_{PSII}/\ \sigma_{PSII'} \times (\bar{a}^{TRON}/\bar{a}^{FT})$, whilst values of *E* were adjusted as *E* x ($\bar{a}^{TRON}/\bar{a}^{FA}$). The $\bar{a}^{FT}$ coefficients applied to measurements in SH were between 0.02 to 0.04 and 0.08 to 0.12 at PH. Values of $\bar{a}^{TRON}$ for SH were 0.02 to 0.05 and 0.09 to 0.13 for PH samples. $\bar{a}^{FA}$ values varied between 0.01 to 0.02 for SH and 0.04 to 0.07 for PH.

Once data was spectrally normalized, carbon fixation rates from each method were normalized to Chl-*a* concentration and photosynthetic-irradiance (P-E) curves were fitted to the hyperbolic tangent equation of Platt et al. (1980). P-E curves were modeled using non-linear squares fit regression analysis in SigmaPlot (ver. 10) to estimate the maximum rate of photosynthesis P_{max} (mg C (mg Chl-*a*)$^{-1}$ h^{-1}), the light utilization efficiency α (mg C (mg Chl-*a*)$^{-1}$ µmol photons^{-1}) and the minimum light saturation parameter E_K (µmol photons m^{-2} s^{-1}) (Jassby and Platt 1976).

2.8. Statistical analyses

Differences in the physicochemical and bio-optical nature of the water types, biomass and photosynthetic traits (P_{max}, E_K, α) of samples were analysed in SPSS Statistics 19 (IBM, New York). Kruskal Wallis tests with Mann-Whitney U *post hoc* tests compared samples using a significance level of 0.05. Repeated measures ANOVA with Bonferroni *post-hoc* tests indicated any changes to $\sigma_{PSII'}$, *C* (1-q*J*) and NPQ with increasing light intensity of the

FRRf steady state light curves. The community structure of phytoplankton (i.e. diagnostic pigments), and the proportion of photosynthetic pigments were compared across sites using non-parametric multivariate analyses of similarity (ANOSIM) and similarity percentage tests (SIMPER) in PRIMER + PERMANOVA (ver. 6.1; Plymouth Marine Laboratories, Plymouth). The correspondence between ^{14}C and FRRf photosynthetic parameters were assessed by linear regression in Origin 9.1 (OriginLab, Massachusetts USA) using the R^2, significance value, fit slope and residuals.

The factors driving the variation in the FRRf and ^{14}C derived photosynthetic parameters were assessed using a distance based redundancy analysis (dbRDA; PRIMER + PERMANOVA; Clark and Warwick 2001). Biological predictors used in this analysis included monovinyl chlorophyll-*a*, proportion of photoprotective pigments (alloxanthin, β-carotene, diatoxanthin, lutein and zeaxanthin, all normalized to the total pigment concentration), proportion of picoplankton and cyanobacteria (using pigment derived estimates). Environmental parameters included temperature, salinity and $K_{d(PAR)}$. Spatial variables included longitude and latitude.

3. Results

3.1. Physicochemical characteristics and bio-optical properties

Temperature was similar within and between locations within the seasonal window of sampling ($p > 0.05$), being 18.8 ± 0.54 °C (mean ± S.E.; $n = 10$) in Sydney Harbour upstream sites and 18.4 ± 0.85 °C ($n = 5$) downstream. At Port Hacking, mean temperature in surface waters was 18.6 ± 0.60 °C ($n = 4$) and 18.1 ± 0.73 °C ($n = 4$) at the sub-surface fluorescence maximum (Table 2). In Sydney Harbour, salinity increased from upstream (29.8 ± 0.94; ($n =$ 10) to downstream (30.4 ± 1.55; $n = 5$; $p < 0.05$) sites and was greatest at Port Hacking ($p <$

0.05), but there was no difference in salinity (PSU) between surface (35.4 ± 0.55; n = 4) and sub-surface samples (34.8 ± 0.55; n = 4; p > 0.05; Table 2). Light attenuation was negatively correlated with salinity and was greatest in the upstream region of Sydney Harbour ($K_{d(PAR)}$ 1.67 m^{-1}), intermediate in lower Sydney Harbour (0.57 m^{-1}) and lowest at Port Hacking (0.07 m^{-1}; p < 0.05) (Table 2). As expected for these coastal locations, wavelength specific differences in light attenuation were observed within and between sites (Table 2). In the upper reaches of Sydney Harbour, blue light ($K_{d(443\ nm)}$ 2.85 m^{-1}) was more heavily attenuated than green ($K_{d(531\ nm)}$ 1.85 m^{-1}) and red light ($K_{d(669\ nm)}$ 1.78 m^{-1}) whilst at the downstream stations there was an increase in green light transmittance ($K_{d(531\ nm)}$ 0.31 m^{-1}) relative to blue ($K_{d(443\ nm)}$ 0.62 m^{-1}) and red ($K_{d(669\ nm)}$ 0.82 m^{-1}). Red as opposed to green or blue light was most attenuated at Port Hacking ($K_{d(669\ nm)}$ 0.20 m^{-1}).

3.2. Phytoplankton community structure

Over the survey period, phytoplankton chlorophyll-*a* concentration was greatest in Sydney Harbour, and was similar between upstream (8.19 ± 1.17 µg L^{-1}; n = 10) and downstream (7.25 ± 1.93 µg L^{-1}; n = 5; p < 0.05; Table 3) sites, but at Port Hacking did not vary between the surface (0.61 ± 0.07 µg L^{-1}; n = 4) and depth of the fluorescence maximum (0.50 ± 0.15 µg L^{-1} n = 4; p > 0.05). According to the diagnostic pigments, the phytoplankton composition differed between locations (Table 3; ANOSIM Global R = 0.692; p = 0.001). Notably, Sydney Harbour was characterized by an increased presence of dinoflagellates (peridinin ~17 % of total Chl-*a* biomass) and at Port Hacking, prochlorophytes (DV Chl-*a* ~16 %) and coccolithophorids (19-Hexanoloxyfucoxanthin ~ 11 %) were prevalent (Table 3). Additionally, the proportion of photosynthetic carotenoid pigments for photosynthesis was higher than their photoprotective counterparts in both Sydney Harbour (PSC: 23 ± 1.3 %; PPC: 7.0 ± 0.5 %) and Port Hacking (PSC: 12 ± 1.0 %; PPC: 9.0 ± 2.0 %) (ANOSIM of

pigment proportions Global R = 0.708; p = 0.029). The same pattern could be seen when comparing the upstream (PSC: 24 ± 1.6 %; PPC: 6.0 ± 0.7 %; $p < 0.05$; n = 10) and downstream (PSC: 20 ± 1.7 %; PPC: 8.0 ± 0.8 %; $p < 0.05$; n = 6) stations in Sydney Harbour. However the proportions of photosynthetic and photoprotective pigments remained constant in the surface (PSC: 10 ± 1.3 %; PPC: 13 ± 2.4 %) and the F_{max} samples (PSC: 14 ± 3.2 %; PPC: 5.0 ± 2.2 %) and did did not differ between populations ($p > 0.05$; n = 8).

3.3. Phytoplankton community photosynthetic traits and productivity

Strong differences were observed in photosynthetic characteristics between sites. Maximum PSII photochemical efficiency, $F_v/F_{m,}$ of phytoplankton assemblages in Sydney Harbour was 10-20 % higher ($p < 0.05$; n = 16) than those at Port Hacking. However there was no significant difference between the surface and sub-surface fluorescence maximum at Port Hacking ($p > 0.05$; n = 8). The functional absorption cross section was ~10% lower in the upstream sites of Sydney Harbour than downstream. Additionally, Sydney Harbour σ_{PSII} was significantly lower than that at Port Hacking ($p < 0.05$; Table 4). The concentration of photochemically active PSII reaction centers [RCII], were generally higher for Sydney Harbour than Port Hacking; however, all measures for [RCII] correlated strongly with corresponding measures of Chl-*a* (n = 23, R^2 = 0.77; Figure 3), suggesting the photosynthetic unit size, mol Chl-*a*:mol RCII was relatively well conserved throughout; notwithstanding, values for mol Chl-*a*: mol RCII were generally higher for Sydney Harbour than for Port Hacking (see Table 4).

Several key patterns in the light response of photochemistry used to determine the ETR_{PSII} were observed for the $Fast^{ACT}$-based FRRF measurements: Values for $\sigma_{PSII'}$ from the phytoplankton assemblages from Sydney Harbour remained steady at most light intensities,

declining slightly at the highest intensity ($p < 0.05$). This is despite an increase in the fraction of closed reaction centres ($p < 0.05$), C (1-qJ) (Figure 2b). In addition, Sydney Harbour samples, both upstream and downstream did not invoke non-photochemical quenching (NPQ was not significantly different with increasing irradiance; $p < 0.05$; Figure 4c). Samples from Port Hacking displayed highly variable function cross sections with increasing irradiance, but no significant trends ($p > 0.05$; Figure 4a). The fraction of closed reaction centres increased consistently with irradiance ($p < 0.05$) however increases in NPQ were not evident until light intensities of >170 µmol photons m^{-2} s^{-1} in both surface and F_{max} samples ($p < 0.05$; Figure 4a, 4c).

Between the two locations, ^{14}C uptake-based chlorophyll-*a* normalized rates of maximum carbon fixation (P_{max}) were greatest at Port Hacking and the upper-most Sydney Harbour site (Table 5). There was no discernible trend in light utilization (α) or the minimum saturating light parameter (E_K) between locations (both $p > 0.05$; Table 5).

FRRf estimates of P_{max}, α and E_K using fluorescence yielded a positive correspondence with values derived using ^{14}C (Figure 5). FRRf-derived estimates of photosynthetic parameters from both sites were positively correlated with independent estimates using ^{14}C carbon fixation (P_{max} : $n = 19$, $R^2 = 0.66$; α : $n = 21$, $R^2 = 0.77$; E_K : $n = 19$, $R^2 = 0.45$; all $p < 0.05$). Given the relatively low absolute estimated values for carbon uptake from the FRRf compared to the ^{14}C incubations, the slopes of the regressions, which are effectively indicative of the error in the assumption of the electron requirement for carbon fixation (since they are multiplied by an assumed 1 O_2 per 4 electrons and a photosynthetic quotient between O_2 evolution and C-uptake of 1.0), were less than unity for both P_{max} and α and only greater than unity for E_K. In all cases, these relationships were significant, thus demonstrating that

electron transport is generally proportional to carbon fixation independent of sampling location or time (Fig. 5).

3.4. Factors driving divergence between FRRf and ^{14}C estimates of P_{max}, α and E_K

A distance based redundancy analysis of the relationship between ^{14}C and FRRf estimates indicated that biological as opposed to spatial and environmental variables were most important in driving the divergence between FRRf and ^{14}C estimates (Table 6a marginal tests; Fig. 6). Despite this, spatial, environmental and biological variables together could explain up to 81% of the variation in photophysiological estimates between samples (Table 6b). The biological parameters which contributed most to explaining the variation in data were chlorophyll-*a* concentration, and relative contribution of picoplankton (pico) and cyanobacteria to total pigment (Uitz et al. 2006; Thompson et al. 2011). According to the marginal tests, the proportion of picoplankton and the phytoplankton biomass (chlorophyll-*a* concentration) were the most important individual parameters contributing to variability in the FRRf:^{14}C relationship (pico $p < 0.001$, Chl-*a* $p = 0.033$). When assessed for the best solution by a single variable, the proportion of picoplankton was again most important (DistLM BEST single solution $R^2 = 0.31$).

4. Discussion

Our study demonstrates a positive correlation between FRRf and ^{14}C estimates of photosynthetic parameters in optically complex coastal waters, suggesting that primary productivity could be estimated with confidence (66%) using FRRf. Overall, the ^{14}C-based rate of phytoplankton biomass production and light utilization by phytoplankton in this study is within the range of other similar turbid estuarine systems studied in temperate areas of the Northern hemisphere (Kinney & Roman 1998; Gamiero et al. 2011) and measurements made

in SE Australian continental shelf waters (Hassler et al. 2011). Paired estimates of the photosynthetic parameters were well correlated with those from FRRf, but there was noticeable non-correspondence with unity, suggesting that the electron requirement for carbon fixation was much lower than expected. A minimum of 4 electrons is required to evolve each molecule of O_2 (and CO_2) (see Suggett et al. 2011 and references therein); although activity of physiological processes such as chlororespiration, the Mehler ascorbate peroxidase reaction, nitrogen reductase cycle as well as photorespiration can elevate this requirement well above 4 (e.g. Suggett et al. 2009); consequently, one would expect values for P_{max} (and α) from FRRf to be at least 4 times greater than those from ^{14}C (ours were a factor of 2 lower). Such unexpectedly low values of productivity for FRRf over ^{14}C have been reported previously (Raatejoa et al. 2004, Lawrenz et al. 2013; see also Boyd et al. 1996) and raise important implications that specific conditions clearly complicate the measurement of electron transport rates using FRRf, and the relationship between electron turnover and carbon uptake.

A general underestimation of photosynthetic rates by FRRf methods in optically complex waters was also seen in Melrose et al. (2006) with the slope of the regression between FRRf and ^{14}C estimates of carbon fixation rates ranging from 0.23 to 1.04, as compared to 0.29 to 2.11 for the photosynthetic parameters measured in this study. A recent metaanalysis of $\Phi_{E:C}$ ratios (determined using predominantly FRRf fluorescence as an estimate of electron transport and ^{14}C incorporation for assessment of carbon fixation) further revealed a global mean of approximately 10 mol electrons per mol C (Lawrenz et al. 2013) but with values routinely below 4 electrons per mol CO_2 fixed for >30% of the studies examined (including many oligotrophic-based studies). Thus "lower than expected" values for FRRf:^{14}C based productivity seems to be a relatively common feature of data sets that have been collected to

date. Such variability may ultimately reflect unmatched time-scales with FRRf- versus ^{14}C-based productivity estimates, i.e., 4 min versus 60 min per light intensity, respectively. Nearly half of the FRRf P_{max} compared to ^{14}C measurements were near or above unity, but the α estimates were generally much lower than unity. Whilst the FRRf productivity at the highest actinic irradiance representing P_{max} was measured after 40 mins of incubation, the FRRf measurements represent α at a much earlier time point (t=4-12 mins). It is possible that due to the temporal separation of measurements that the physiological pathways responsible for the (de-)coupling of electron transport and carbon uptake (above) are activated/de-activated at different timepoints in the FRRf and ^{14}C measurements. However, the frequent occurrence of relatively low FRRf: ^{14}C values is more difficult to explain but may represent sources of operational error (Lawrenz et al. 2013).

Major potential sources of error in calculating absolute ETRs via FRRf arise from a lack of knowledge of functional [RCII], and accuracy of the light intensities used for excitation, both actinic for the light curve determination but also the saturation flashlets used to derive σ_{PSII} (Suggett et al. 2009b, Oxborough et al. 2012). Our approach used values of [RCII] that were calibrated against independent measurements and the LED intensity within the *FAST*^{ACT} verified with independent PAR measurements and thus we can discount the first two possibilities. However, the values of σ_{PSII} that we determined with the *Fast*^{TRACKA} *MKII* (~ 200 and 400 for SH and PH, respectively) appear lower by a factor of 1.5-2, where dominated by dinoflagellates and/or prochlorophytes/coccolithophores, compared to values determined by older generation FRR fluorometers (see Suggett et al. 2009b). Such differences are of course difficult to confidently state as a source of error given the potential role of photoacclimation and nutrient status in further modifying 'specific-specific signatures' of σ_{PSII} (Suggett et al. 2009b). However, the source of error inherent to σ_{PSII} can effectively be

removed by considering an alternative FRRf-based productivity algorithm (Oxborough et al. 2012).

The use of an "absorption" based algorithm as derived by Oxborough et al. (2012) removes the need for including the $\sigma_{PSII'}$ (where measurements become mathematically unreliable in actinic light) and for the choice of model describing connectivity (puddle vs lake model – i.e. no connectivity vs maximum connectivity). Comparing Eq. 5 using our "sigma-based" versus the "absorption based" method for our data sets demonstrated approximately up to 15% higher values of carbon fixation for the absorption than sigma based method for Sydney Harbour data (R^2 = 0.98; slope = 1.13 ± 0.01; $p < 0.05$), and up to 14 difference either side of the unity line for the Port Hacking data (R^2 = 0.83; slope = 1.04 ± 0.05; $p < 0.05$) (Figure 2b). The absorption method does not appear to improve the relationship between FRRf and ^{14}C estimates, i.e. the predictability of FRRf to estimate primary production, as indicated by no change in output (R^2) of linear regressions for each photosynthetic parameter (see Table 7). However the quantum requirement, $\Phi_{E:C}$ has changed considerably (see Table 7). The absorption algorithm has elevated values of FRRf based productivity (as expected by Oxborough et al. 2012). The greatest improvement in quantum requirement is seen in the Port Hacking samples, which may suffer from the use of the sigma method since these data appear to reflect increased variability in $\sigma_{PSII'}$ and fraction of closed reaction centres with increasing actinic light (Fig. 2). Routine use of an absorption (non-sigma) based approach may thus provide a means to more reliably and accurately evaluate $\Phi_{E:C}$ in future studies.

Despite the difficulties in reconciling the absolute FRRF and ^{14}C productivity values, it is still evident from our data that the slope between FRRf and ^{14}C productivity was two-fold higher for P_{max} than α. It is acknowledged here that despite the Platt "PvI" curve fitting model

converging for all ^{14}C and FRRf estimates (^{14}C $p < 0.01$, $R^2 = 0.60 – 0.95$; FRRf $p < 0.01$, $R^2 = > 0.95$), there is a empirical uncertainty in the derivation of either alpha or P_{max} in the two techniques, which can ultimately translate to the calculation of $E_{K,}$ which is the ratio of P_{max} to α. The ^{14}C method lacks resolution of data points in the lower light intensities required to derive reliable alpha values (Boyd et al. 1997), and in this study, the FRRf failed to reach saturating irradiance, which MacIntyre et al. (2002) reports can have implications for robust estimates of P_{max}. The result of both types of these uncertainties is potential error propagation in the calculation of E_K using both the ^{14}C tracer and fluorescence approaches.

The meta-analysis by Lawrenz et al. (2013) showed that geographically specific ratios were highly variable and largely driven by environmental parameters such as temperature, K_d and nutrient concentrations (Lawrenz et al. 2013). We observed low variability in temperature, but a large gradient in K_d and significantly higher nutrient concentrations within Sydney Harbour than at Port Hacking (Doblin et al. unpublished data). Within the Port Jackson estuary, nutrient concentrations are highly driven by dry weather base-flow from the surrounding catchment as opposed to freshwater inputs during high rainfall events (Hedge et al. 2013). As a result, it is hard to infer any specific relationship between salinity or temperature and dissolved nutrient concentrations. Regardless of the clear differences in environmental variables, the distance based redundancy analysis in this study revealed greater significance of biological variables driving divergence in fluorescence-based compared to ^{14}C estimates of primary production. The co-variance of phytoplankton composition with changes in light, temperature and nutrients is a strong explanation as to why Lawrenz et al (2013) did not explicitly identify phytoplankton composition as being an important driver of variability in $\Phi_{E:C}$.

Phytoplankton composition, specifically the proportion of picoplankton, and Chl-*a* biomass appeared highly significant in explaining the variance between FRRf and ^{14}C estimates for our study. Increased concentrations of diagnostic pigments for cyanobacteria (zeaxanthin and DV-Chlorophyll-*a*) were found at Port Hacking, indicating increased cyanobacterial presence. Interestingly, relatively low productivity values for FRRf compared to ^{14}C-uptake from Raatejoa et al (2004) in the Baltic Sea and Suggett et al. (2001) in the north-east Atlantic both corresponded with periods of cyanobacterial dominance (see Suggett et al. 2009a also). Most likely these may reflect "underestimates" of electron transport rates by the FRRf approach used here (and previously), where excitation (and hence fluorescence emission) is not spectrally resolved.

Whilst not explicitly tested in this study, previous studies have noted that the presence of cyanobacteria complicate the interpretation of fluorescence signals (Raateoja et al. 2004; Frenette et al. 2012; Schreiber et al. 2012; Silsbe et al. 2012; Simis et al. 2012) due to their naturally low quantum yield of fluorescence (when measured with a blue excitation source). This is primarily as a result of most Chl-*a* being attached to the PSI (not PSII) antennae (Campbell et al. 1998), but may be exacerbated due to differences in the pigment antennae and wavelength dependent optical absorption cross section (α_{phy^*}), resulting in peak absorption different to most fluorometer excitation wavelengths (see Blache et al. 2011; Schreiber et al. 2012). Such artifacts thus carry implications for determining the true minimum saturation point and maximum rate of photosynthesis for many phytoplankton species. In acknowledging the problem, Ralph and co-workers recently used a submersible fluorometer with both blue and red LED sources to resolve the cyanobacterial influence on *in situ* fluorescence signals at two stations in the Tasman Sea. At an oligotrophic station with a deep Chl-*a* maximum (90-100 m), the F_v/F_m derived from the red channel (indicative of

cyanobacteria) was lower than the F_v/F_m in the blue channel (total phototrophic community), and this was consistent with the vertical distribution of pigments diagnostic for cyanobacteria, as well as flow cytometrically determined *Synechococcus* abundance (Hassler et al. 2013 in press). We also observed lower values of F_v/F_m at Port Hacking than SH; however, these lower values corresponded with higher values for σ_{PSII} that, for a blue excitation source such as the *Fast*^{TRACKA} *MKII*, would not necessarily be consistent with a shift to cyanobacteria (see Suggett et al. 2009b) unless cells were simultaneously photoinhibited. Here we accounted for the differences between instrument actinic light sources supplying incubation and measuring light and also any spectral biases of fluorescent excitation towards particular species by correcting all estimates using the α_{phy^*}.

An overall lack of "control" of the environment, relative to the community structure, in determining the coupling between FRRf and ^{14}C estimates of productivity was further evidenced through the additional photophysiological parameters. In addition to the relationship between F_v/F_m and σ_{PSII} (above), photosynthetic parameters (namely α and E_K) did not reflect acclimation to the specific bio-optical conditions measured in either location at the time of sampling. In Brading et al. (2013) higher values of $\Phi_{E:C}$ for P_{max} than α values were attributed to the up-regulation of alternative energy dissipation pathways under light saturation. Similar to Brading et al. (2013) we also report higher estimates for E_K from FRRf than ^{14}C uptake indicating that alternative electron sinks may be in operation or NPQ is highly activated (Moore et al. 2006; Halsey et al. 2013). Water residence time within Sydney Harbour has been reported to be within 0 and 20 days in the main lower channel of the harbour, and up to 130 days in the upper reaches of the Parramatta River (Hedge et al. 2013). Similarly, at Port Hacking water residence time which exceeds phytoplankton division rates is also common due to stratification of the water column (Rendell & Pritchard 1996). Despite

the time exposed to a particular high or low light environment theoretically exceeding that of cell doubling time, this study found there is little evidence of acclimation to the *in situ* light environment.

Fluorescence derived estimates of [RCII] used in the sigma algorithm of this study were strongly correlated with chlorophyll-*a* concentration. However, chlorophyll-*a* was not a good biological indicator for total production estimates in this system; no doubt the presence of non-algal particles and photoacclimation would be important in driving divergence. However chlorophyll-*a* was identified as a key parameter explaining variability between FRRf and ^{14}C estimates. The calculation of [RCII] using the relationship between the minimum fluorescence parameter (F_0) and [RCII] as determined by Oxborough et al. (2012) may be sensitive to nutrient stress (C.M. Moore *pers. comm.*) which results in the enhanced uncoupling of chlorophyll complexes and PSII reaction centres and poor estimation of electron transport. Despite all best efforts to bring phytoplankton samples to a fully relaxed dark adapted state, the residual effects of light induced fluorescence quenching on the F_0 (or $[Chl]^{FRRf}$ in this case) may last for several hours after phytoplankton are removed from a saturating light environment. Hence this fluorescence quenching may affect fluorescence estimates of [RCII] through either quenching of the F_0 at the time of measurements, or variability in the assumed (constant) relationship between the kinetic coefficiencts of fluorescence (k_f) and photochemistry (k_p) (K. Oxborough *pers. comm.*). Other important methodological factors potentially contributing the measurement of minimum fluorescence include non-algal particles which act to attenuate light and are naturally fluorescent. The methods practiced in this study make all best efforts to account for biases in the fluorescence measurements due to the presence of various light absorbing samples in the sample and differences in the light sources used. Additionally it is acknowledged that the approach

outlined by Lawrenz et al. (2013) where FRRf and ^{14}C measurements were performed on the same sample in the *Fast*^{ACT} may work towards further eliminating such biases (Lawrenz et al. 2013).

5. Conclusion.

The application of fluorometry to derive estimates of primary productivity has advanced significantly since its inception (Kolber & Falkowski 1993) and our study aimed to test the robustness of newly developed FRRf algorithms in more optically complex waters. As with previous studies (Lawrenz et al. 2013), it is clear that the relationship between FRRf and ^{14}C-uptake based productivity rates is highly dependent on the system in question and thus the underlying environmental and taxonomic conditions; even so, relationships can be identified to link FRRf from (and therefore potentially utilize it to predict) CO_2 uptake rates. Of major importance is to better identify why FRRf estimates of carbon uptake are frequently "lower than expected". This study has shown that a push towards identifying the role of taxonomy (and in particular cyanobacteria) is clearly warranted, e.g. through spectrally resolved fluorometry or laboratory-based studies on monocultures under controlled conditions. We also need to better understand the timescales at which physiological pathways operate that de-couple electron transport rates to CO_2-uptake, and to identify how best to reconcile differences with the underlying environmental history which natural phytoplankton communities experience in dynamic coastal systems. Such studies are critically needed to enable developments in FRRf (and associated productivity algorithm development) to be best applied.

6. Acknowledgements

The authors acknowledge the assistance of L. Clementson and J. Everett in data processing and the use of optical instrumentation owned by the Sydney Institute of Marine Science. CR is supported by a CSIRO Australia Wealth from the Oceans Flagship top-up scholarship and a UTS Plant Functional Biology and Climate Change Cluster scholarship. This research forms part of the CSIRO funded Marine and Coastal Carbon Biogeochemistry Cluster.

7. References

Barlow, R.G., Aiken, J., Moore, G.F., Holligan, P.M. & Lavender, S. 2004, 'Pigment adaptations in surface phytoplankton along the eastern boundary of the Atlantic Ocean', *Marine Ecology Progress Series*, vol. 281, pp. 13-26.

Blache, U., Jakob, T., Su, W. & Wilhelm, C. 2011, 'The impact of cell-specific absorption properties on the correlation of electron transport rates measured by chlorophyll fluorescence and photosynthetic oxygen production in planktonic algae', *Plant Physiology and Biochemistry*, vol. 49 no. 8, pp. 801-8.

Boyd, P.W., Aiken, J. & Kolber, Z. 1997, 'Comparison of radiocarbon and fluorescence based (pump and probe) measurements of phytoplankton photosynthetic characteristics in the Northeast Atlantic Ocean', *marine Ecology progress Series*, vol. 149, pp. 215-226.

Brading, P., Warner, M.E., Smith, D.J. & Suggett, D.J. 2013, 'Contrasting modes of inorganic carbon acquisition amongst Symbiodinium (Dinophyceae) phenotypes', *New Phytologist*, vol. 200, no. 2, pp. 432-442.

Campbell, D., Hurry, V., Clarke, A.K., Gustafsson, P. & Oquist, G. 1998, 'Chlorophyll fluorescence analysis of cyanobacterial photosynthesis and acclimation', *Microbiology and Molecular Biology Reviews*, vol. 63, no. 3, pp 667–683.

Clarke, K.R. & Warwick, R.M. 2001, *Change in marine communities: an approach to statistical analysis and interpretation*, PRIMER-E, Plymouth.

Falkowski, P.G. 2012, 'The power of the plankton', *Nature*, vol. 438, pp. 517-20.

Frenette, J.J., Massicotte, P. & Lapierre, J.F. 2012, 'Colorful niches of phytoplankton shaped by the spatial connectivity in a large river ecosystem: A riverscape perspective', *PLoS One*, vol. 7, no. 4, pp. e5891.

Fujuki, T., Suzue, T., Kimoto, H. & Saino, T. 2007, 'Photosynthetic electron transport in *Dunaliella tertiolecta* (Chlorophyceae) measured by fast repetition rate fluorometry: relation to carbon assimilation', *Journal of Plankton Research*, vol. 29, no. 2, pp199-208.

Gameiro, C., Zwolinski, J. & Brotas, V. 2011, 'Light control on phytoplankton production in a shallow and turbid estuarine system', *Hydrobiologia*, vol. 669, pp. 249-263.

Hasley, K.H., O'Malley, R.T., Graff, J.R., Milligan, A.J. & Behrenfeld, M.J. 2013, 'A common partitioning strategy for photosynthetic products in evolutionary distinct phytoplankton species', *New Phytologist*, vol. 198, pp. 1030-38.

Hassler, C.S., Djajadikarta, J.R., Doblin, M.A, Everett, J.D. & Thompson, P.A. 2011, 'Characterisation of water masses and phytoplankton nutritient limitation in the East Australian Current separation zone during spring 2008', *Deep Sea Research Part II: Topical Studies in Oceanography*, vol. 58, no. 5, pp. 664-77.

Hedge, L., Johnston, E., Birch, G., Booth, D., Creese, B., Doblin, M., Figueira, W., Gribben, P., Hutchings, P., Mayer Pinto, M., Marzinelli, E., Pritchard, T. & Steinberg, P. 2013, *Living Harbour. Dynamic science: A systematic review of the science of Sydney Harbour*, Sydney Institute of Marine Science, Sydney Australia, ISBN: 978-0-646-91693-0, Publisher: The Sydney Institute of Marine Science, Sydney, New South Wales, Australia

Jassby, A.D. & Platt, T. 1976, 'The relationship between photosynthesis and light for natural assemblages of coastal marine phytoplankton', *Journal of Phycology*, vol. 12, pp. 421-30.

Kaiblinger, C. & Dokulil, M.T. 2006, 'Application of fast repetition rate fluorometry to phytoplankton photosynthetic parameters in freshwaters', *Photosynthesis Research*, vol. 88, pp. 19-30.

Kinney, E.H., & Roman, C.T. 1998, 'Response of primary producers to nutrient enrichment in a shallow estuary', *Marine Ecology Progress Series*, vol. 163, pp. 89-98.

Kirk, J.T.O. 2011, *Light and Photosynthesis in Aquatic Ecosystems*, 3rd edn, Cambridge University Press, Cambridge.

Knap, A. H., Michaels, A., Close, A. R., Ducklow, H., & Dickson, A. G. 1996, 'Protocols for the joint global ocean flux study (JGOFS) core measurements', *JGOFS, Reprint of the IOC Manuals and Guides No. 29, UNESCO 1994*, 19.

Kolber, Z. & Falkowski, P.G. 1993, 'Use of active fluorescence to estimate phytoplankton photosynthesis in situ', *Limnology and Oceanography*, vol. 38, no. 8, pp. 1646-65.

Kolber, Z.S., Prasil, O. & Falkowski, P.G. 1998, 'Measurement of variable chlorophyll fluorescence using fast repetition rate techniques: defining methodology and experimental protocols', *Biochimica et Biophysica Acta*, vol. 1367, no. 1, pp. 88-106.

Kromkamp, J.C., Dijkman, N.A., Peene, J., Simis, S.G.H. & Gons, H.J 2008, 'Estimating phytoplankton primary production in Lake Ijsselmeer (The Netherlands) using variable fluorescence (PAM-FRRF) and C-uptake techniques', *European Journal of Phycology*, vol. 43, no. 4, pp. 327-344.

Lawrenz, E., Pinckney, J.L., Ranhofer, M.L., MacIntyre, H.L. & Richardson, T.L. 2010, 'Spectral irradiance and phytoplankton community composition in a blackwater-dominated estuary, Winyah Bay, South Carolina, USA', *Estuaries and Coasts*, vol. 33, no. 5, pp. 1186-1201.

Lawrenz, E., Silsbe, G., Capuzzo, E., Ylostalo, P., Forster, R.M., Simis, S.G.H., Prasil, O., Kromkamp, J., Hickman, A.E., Moore, C.M., Forget, M-H., Geider, R. & Suggett, D.J. 2013, 'Predicting the electron requirement for carbon fixation in seas and oceans', *PLOS One*, vol. 8, no. 3. Pp. e58137.

Lawrenz, E., Huete-Ortega, M., Suggett, D.J. & Geider, R.J. 2013, May, 'The effect of

nitrogen-limitation on the electron requirement for carbon fixation in marine phytoplankton', Poster presented at the *45th Liege Colloquium: The variability of primary production in the ocean: from the synoptic to the global scale*, Liege, Belgium.

Lewis, M.R., Smith, J.C. 1983, 'A small volume, short-incubation-time method for measurement of photosynthesis as a function of incident irradiance', *Marine Ecology Progress Series*, vol. 13, pp. 99-102.

Lee, S.B., Birch, G.F. & Lemckert, C.J. 2011, 'Field and modeling investigations of fresh-water plume behavior in response to infrequent high-precipitation events, Sydney Estuary, Australia', *Estuarine, Coastal and Shelf Science*, vol. 92, pp. 389-402.

MacIntyre, H.L., Kana, T.M. & Geider, R.J. 2000, 'The effect of water motion on short-term rates of photosynthesis by marine phytoplankton', *Trends in Plant Science*, vol. 5, no. 1, pp. 12-17.

MacIntyre, H.L., Kana, T.M., Anning, T. & Geider, R.J. 2002, 'Photoacclimation of photosynthesis irradiance response curves and photosynthetic pigments in microalgae and cyanobacteria', *Journal of Phycology*, vol. 38, pp. 17-38.

Marra, J. 2002, 'Approaches to the measurement of plankton production', in P.J. LeB. Williams, D.N. Thomas & C.S. Reynolds (eds.), *Phytoplankton productivity: Carbon assimilation in marine and freshwater ecosystems*, Black-well Science Inc., Oxford, pp. 78-108.

Melrose, D.C., Oviatt, C.A., O'Reilly, J.E. & Berman, M.S. 2006, 'Comparisons of fast repetition rate fluorescence estimated primary production and ^{14}C uptake by phytoplankton', *Marine Ecology Progress Series*, vol. 311, pp. 37-46.

Mitchell, B. G., Kahru, M., Wieland, J., & Stramska, M. (2002). Determination of spectral absorption coefficients of particles, dissolved material and phytoplankton for discrete

water samples. *Ocean optics protocols for satellite ocean color sensor validation, Revision, 3*, 231-257

Moore, M.C., Suggett, D.J., Hickman, A.E., Kim, Y-N., Tweddle, J.F., Sharples, J., Geider, R. & Holligan, P.M. 2006, 'Phytoplankton photoacclimation and photoadaption in response to environmental gradients in a shelf sea', *Limnology and Oceanography*, vol. 51, no. 2, pp. 936-49.

Napoleon, C. & Claquin, P. 2012, 'Multi-parametric relationships between PAM measurements and carbon incorporation, an *in situ* approach', *PLOS One*, vol. 7, no. 7, pp. 1-12.

Oxborough, K., Moore, C.M., Suggett, D.J., Lawson, T., Chan, H.G. & Geider, R.J. 2012, 'Direct estimation of functional PSII reaction centre concentration and PSII electron flux on a volume basis: a new approach to the analysis of Fast Repetition Rate fluorometry (FRRf) data', *Limnology and Oceanography: Methods*, vol. 10, pp. 142-54.

Platt, T., Gallegos, C.L. & Harrison, W.G. 1980, 'Photoinhibition of photosynthesis in natural assemblages of marine phytoplankton', *Journal of Marine Research*, vol. 38, vol. 4, pp. 687-701

Prieto, L., Vaillancourt, R.D., Hales, B. & Marra, J. 2008, 'On the relationship between carbon fixation efficiency and bio-optical characteristics of phytoplankton', *Journal of Plankton Research*, vol. 30, no. 1, pp. 43-56.

Pritchard, T., Lee, R., Ajani, P., Rendell, P. & Black, K. 2001, 'How do ocean outfalls affect nutrient patterns in coastal waters of New South Wales, Australia?', *Journal of Coastal Research*, vol. 34, pp. 96-109.

Pritchard, T.R, Lee, R.S., Ajani, P.A., Rendell, P.S., Black, K. & Koop, K. 2003, 'Phytoplankton responses to nutrient sources in coastal waters off Southeastern Australia', *Aquatic Ecosystem Health & Managament*, vol. 6, no. 2, pp. 105-17

Raateoja, M., Seppala, J. & Ylostalo, P. 2004, 'Fast repetition rate fluorometry is not applicable to studies of filamentous cyanobacteria from the Baltic Sea', *Limnology and Oceanography*, vol 49, no. 4, pp. 1006-12.

Rendell, P.S. & Pritchard, T.R. 1996, 'Physicochemcical conditions in coastal waters off Sydney, Central NSW, Australia', *Marine Pollution Bulletin*, vol. 33, no. 7-12, pp. 132-39.

Schreiber, U., Klughammer, C. & Kolbowski, J. 2012, 'Assessment of wavelength-dependent parameters of photosynthetic electron transport with a new type of multi-color PAM chlorophyll fluorometer', *Photosynthesis Research*, vol. 113, pp. 127-144.

Silsbe, G.M. & Kromkamp, J.C. 2012, 'Modelling the irradiance dependency of the quantum efficiency of photosynthesis', *Limnology and Oceanography: Methods*, vol. 10, pp. 645-52.

Simis, G.H., Huot, Y., Babin, M., Seppala, J. & Metsamaa, L. 2012, 'Optimization of variable fluorescence measurements of phytoplankton communities with cyanobacteria', *Photosynthesis Research*, vol. 112, pp. 13-30.

Smyth, T.J., Pemberton, K.L., Aiken, J. & Geider, R.J. 2004, 'A methodology to determine primary production and phytoplankton photosynthetic parameters from Fast Repetition Rate fluorometry', *Journal of Plankton Research*, vol. 26, no. 11, pp. 1337-50.

Suggett, D.J., Oxborough, K., baker, N.R., MacIntyre, H., Kana, T.M. & Geider, R. 2003, 'Fast repetition rate and pulse amplitude modulation chlorophyll a fluorescence

measurements for assessment of photosynthetic electron transport in marine phytoplankton', *European Journal of Phycology*, vol. 38, no. 4, pp. 371-84.

Suggett, D.J., MacIntyre, H.L. & Geider, R.J. 2004, 'Evaluation of biophysical and optical determinations of light absorption by photosystem II in phytoplankton', *Limnology and Oceanography: Methods*, vol. 2, pp. 316-32.

Suggett, D.J., Moore, C.M., Maranon, E., Omachi, C., Varela, R., Aiken, J. & Holligan, P.M. 2006, 'Photosynthetic electron turnover in the tropical and subtropical Atalantic Ocean', *Deep-Sea Research II*, vol. 53, pp. 1573-92.

Suggett, D.J., MacIntyre, H.L. Kana, T.M. & Geider, R.J.2009a, 'Comparing electron transport with gas exchange parameterizing exchange rates between alternative photosynthetic currencies for eukaryotic phytoplankton', *Aquatic Microbial Ecology*, vol. 56, pp. 147-62.

Suggett, D.J., Moore, C.M., Hickman, A.E. & Geider, R.J. 2009b, 'Interpretation of fast repetition rate (FRR) fluorescence signatures of phytoplankton community structure versus physiological state', *marine Ecology Progress Series*, vol. 376, pp. 1-19.

Suggett, D.J., Borowitzka, M.A. & Prasil, O. 2011 *Chlorophyll a fluorescence in aquatic sciences: Methods and applications*, Springer Science and Business Media, New York.

Steeman Nielsen E. 1952, 'The use of radioactive carbon (C14) for measuring organic production in the sea', *Journal Du Coneils Permanent International pour l'Exploration de la Mer*, vol. 18, pp. 117-40.

Tassan, S. & Ferrari, G.M. 1995, 'An alternative approach to absorption measurements of aquatic particles retained on filters', *Limnology and Oceanography*, vol. 40, no. 8, pp. 1358-68.

Taylor, B.B., Torrecilla, E., Bernhardt, A., Taylor, M.H., Peeken, I., Rottgers, R., Piera, J. & Bracher, A. 2011, 'Bio-optical provinces in the eastern Atlantic Ocean and their biogeographical relevance', *Biogeosciences*, vol. 8, pp. 3609-629.

Thompson, P.A., Bohnam, P., Waite, A.M., Clementson, L.A., Cherukuru, N., Hassler, C. & Doblin, M.A. 2011, 'Contrasting oceanographic conditions and phytoplankton communities on the east and west coasts of Australia', *Deep-Sea Research II*, vol. 58, pp. 645-663.

Uitz, J., Claustre, H., Morel, A. & Hooker, S.B. 2006, 'Vertical distribution of phytoplankton communities in open ocean: An assessment based on surface chlorophyll', *Journal of Geophysical Research: Oceans*, vol. 111 no. C8, pp. 1978-2012.

Van Heukelem, L. & Thomas, C.S. 2001, 'Computer-assisted high-performance liquid chromatography method development with applications to the isolation and analysis of phytoplankton pigments', *Journal of Chromatography A*, vol.910, pp 31-49.

Tables

Table 1: Variables measured and applied in this study to derive FRRf-based estimates of primary productivity.

Variable	Definition
PC_{FRR}	rate of gross photosynthesis (mg C (mg Chl-*a*)$^{-1}$ hr^{-1})
E	photosynthetically active radiation (400 – 700 nm) (µmol photons m^{-2} s^{-1}) of light (wavelength dependent)
σ_{PSII}	functional absorption cross section nm^2 quanta^{-1}
$\sigma_{PSII'}$	functional absorption cross section nm^2 quanta^{-1} in actinic light
1- *C*	fraction of open reaction centres (C = 1-q*J*)
PSU	photosynthetic unit size is the concentration of functional PSII reaction centres (mol Chl-*a* m^{-3}/ mol RCII m^{-3})
[RCII]	Number of functional reaction centres (mol RCII m^{-3}) = $\frac{K_R}{E_{LED}}$ x $\frac{[Chl]^{FRRf}}{\sigma_{PSII}}$
$[Chl]^{FRRf}$	gain normalized minimum fluorescence signal parameter calculated by *FastPro*
K_R	instrument specific constant (mol photons m^{-3} s^{-1})
$\Phi_{E:C}$	electron requirement for carbon uptake (molecule CO_2 (mol electrons)$^{-1}$)

Table 2: Physicochemical and bio-optical characteristics of sampling sites in Sydney Harbour and Port Hacking.

	Sydney Harbour upstream	Sydney Harbour downstream	Port Hacking surface	Port Hacking sub-surface fluorescence maximum
Temperature (°C)	18.8 ± 0.54	18.4 ± 0.85	18.6 ± 0.60	18.1 ± 0.73
Salinity	29.8 ± 0.94	30.4 ± 1.55	35.4 ± 0.06	34.8 ± 0.55
Chl-*a* (μg L^{-1})	8.19 ± 1.17	7.25 ± 1.93	0.61 ± 0.07	0.50 ± 0.15
K_d PAR (m^{-1})	1.67 ± 0.12	0.57 ± 0.22	0.08 ± 0.03	0.08 ± 0.03

Wavelength attenuation coefficient K_d (λ) (m^{-1})	Sydney Harbour upstream	Sydney Harbour downstream	Port Hacking
443 nm	2.85	0.62	0.05
531 nm	1.87	0.31	0.07
669 nm	1.78	0.82	0.20

Table 3: Phytoplankton community pigments (normalized to mono-vinyl chlorophyll-*a* and presented as %) across all sites, including the mean ± S.E. of diagnostic pigments and the mean proportion of photosynthetic and photoprotectve pigments. Diagnostic pigments are indicative of the presence of particular phytoplankton species. Note that Peridinin = dinoflagellates, 19'-butanoloxyfucoxanthin = pelagophytes, Fucoxanthin ≈ diatoms, Prasinoxanthin = prasinophytes, Neoxanthin + Violaxanthin + Lutein + Chlorophyll-*b* ≈ chlorophytes, 19'-Hexanoloxyfucoxanthin ≈ Coccolithophorids, Alloxanthin ≈ Cryptophytes, Zeaxanthin ≈ *Synechococcus* sp. and Divinyl chlorophyll-*a* = *Prochlorococcus* sp. (Values marked with * are below detection limits of the method)

Pigment concentration (normalized to MV-Chl-*a*) ($x10^{-2}$ µg L^{-1})	**Sydney Harbour upstream**	**Sydney Harbour downstream**	**Port Hacking surface**	**Port Hacking sub-surface fluorescence maximum**
Peridinin	16.9 ± 4.18	5.72 ± 1.55	0.73 ± 0.47	0.00 ± 0.00
19'-Butanoloxyfucoxanthin	0.82 ± 0.34	0.32 ± 0.32*	2.99 ± 0.57	4.35 ± 2.85
Fucoxanthin	19.4 ± 1.76	19.9 ± 2.22	7.26 ± 1.08	17.0 ± 4.75
Prasinoxanthin	0.71 ± 0.21	3.00 ± 0.65	2.77 ± 0.35	1.36 ± 0.59
Neoxanthin	1.55 ± 0.29	2.62 ± 0.27	1.90 ± 0.87	6.70 ± 4.10
Violaxanthin	2.12 ± 0.22	3.68 ± 0.59	0.92 ± 0.06	0.82 ± 0.65
Lutein	0.38 ± 0.21*	0.21 ± 0.21*	1.99 ± 0.56	0.00 ± 0.00*
Chlorophyll-*b*	12.3 ± 0.96	16.8 ± 0.91	20.7 ± 3.47	7.88 ± 2.66
19'-Hexanoloxyfucoxanthin	0.23 ± 0.16*	1.33 ± 0.55	9.51 ± 0.89	3.60 ± 1.25
Alloxanthin	2.78 ± 0.32	6.50 ± 0.10	2.60 ± 0.35	1.15 ± 0.80
Zeaxanthin	3.80 ± 1.06	3.60 ± 1.11	8.75 ± 2.50	1.33 ± 0.68
Divinyl chlorophyll-*a*	1.77 ± 0.62	0.24 ± 0.24*	3.7 ± 0.87	23.4 ± 0.52

Table 4: Photosynthetic parameters, including F_v/F_m, and σ_{PSII} from instantaneous fluorescence measurements, [RCII], and the photosynthetic unit size (PSU) calculated using the method by Oxborough et al. (2012). Values reported are the mean ± S.E.

Site	**F_v/F_m**	**σ_{PSII} (nm^{-2})**	**[RCII] (mol RCII m^{-3}) (x 10^{-9})**	**PSU (mol Chl-*a*/mol RCII)**
Sydney Harbour upstream	0.435 ± 0.024	2.47 ± 0.12	19.3 ± 2.97	591 ± 65.2
Sydney Harbour downstream	0.435 ± 0.034	2.68 ± 0.10	9.63 ± 0.97	581 ± 11.2
Port Hacking surface	0.357 ± 0.015	4.13 ± 0.23	1.96 ± 0.53	308 ± 30.7
Port Hacking sub-surface F_{max}	0.400 ± 0.015	3.78 ± 0.14	1.86 ± 0.58	397 ± 10.0

Table 5. Photosynthetic parameters derived using ^{14}C and FRRf. Parameters include the maximum photosynthetic rate (P_{max}), light utilization efficiency (α) and light saturation parameter (E_k). Values are mean ± SE.

Site	Station	*n*	P_{max} (mg C (mg chl-a)$^{-1}$ hr^{-1})		α (mg C (mg chl-*a*)$^{-1}$ µmol photons^{-1})		E_k (µmol photons m^{-2} s^{-1})	
					(x 10^{-2})	(x 10^{-3})		
			^{14}C	FRRf	^{14}C	FRRf	^{14}C	FRRf
Sydney Harbour Upstream	1	2	4.32 ± 1.05	0.90 ± 0.73	1.67 ± 0.04	3.20 ± 0.47	258 ± 57.0	542 ± 48.7
	2	2	2.08 ± 0.05	2.13 ± 1.86	1.13 ± 0.22	3.35 ± 0.35	191 ± 32.9	941 ± 293
	3	2	2.37 ± 0.15	1.47 ± 0.73	1.67 ± 0.14	3.66± 0.13	143 ± 2.35	545 ± 395
	4	2	n.d.	0.89 ±0.06	n.d.	2.91 ± 0.06	n.d.	321 ± 85.0
	5	2	1.03 ± 0.43	0.74 ± 0.50	1.86 ± 0.86	4.20 ± 1.37	75.7 ± 22.3	435 ± 1.00
Sydney Harbour Downstream	6	2	1.36 ± 0.05	1.09± 0.66	1.31 ± 0.04	3.57 ± 0.94	104 ± 6.52	332 ± 107
	7	1	n.d.	1.01 ± 0.00	n.d.	4.87 ± 0.00	n.d.	208 ± 0.00
	8	2	0.79 ± 0.08	1.23 ± 0.22	1.03 ± 0.44	5.27 ± 2.85	88.6 ± 29.9	299 ± 120
Port Hacking Surface	-	4	3.5 ± 1.2	1.91 ± 0.97	3.68 ± 1.25	10.2 ± 4.21	111 ± 26.0	187 ± 50.7
Port Hacking sub-surface F_{max}	-	4	3.6 ± 1.2	1.76 ± 0.33	3.10 ± 0.99	14.1 ± 2.24	122 ± 11.7	135 ± 32.5

Table 6. a) Contribution of spatial, environmental and biological parameters to variability in the relationship between FRRf and ^{14}C estimates of primary productivity. **b)** Overall best solutions for describing dissimilarity between samples**. (**Lo = longitude, La = latitude, T = temperature, Sal = salinity, K_d = K_dPAR, Chl = MV Chl-*a* PPC = proportion of photoprotective pigment, Pico = picoplankton proportion, Cyano = proportion of cyanobacteria.)

a. Marginal tests

Predictor Variable	SS (Trace)	P	Proportion
Spatial	10.9	0.130	0.201
Environmental	11.0	0.291	0.203
Biological	24.0	**0.018**	0.444
Latitude	9.08	0.051	0.168
Longitude	4.75	0.205	0.081
Temperature	7.92	0.051	0.147
Salinity	5.50	0.157	0.102
K_d	4.33	0.231	0.080
Chlorophyll-*a*	9.40	**0.033**	0.174
PPC	2.68	0.408	0.050
Picoplankton	16.9	**0.001**	0.309
Cyanobacteria	6.02	0.140	0.111

b. Overall best solutions

Best solutions for each number of variables		
No. of predictor variables	**Variables**	**R^2**
1	Pico	0.309
2	Pico, Cyano	0.424
3	Lo, Pico, Cyano	0.515
4	Lo, Chl, Pico, Cyano	0.648
5	Lo, Sal, Chl, Pico, Cyano	0.681
6	Lo, T, Sal, Chl, Pico, Cyano	0.714
7	La, Lo, T, Sal, Chl, Pico, Cyano	0.747
8	La, Lo, T, Sal, Chl, PPC, Pico, Cyano	0.772
9	Lat, Lo, T, Sal, K_d, Chl, PPC, Pico, Cyano	0.781

Overall best solutions		
No. of predictor variables	**Variables**	**R^2**
7	La, Lo, T, Sal, Chl, Pico, Cyano	0.747
8	La, Lo, T, Sal, Chl, PPC, Pico, Cyano	0.772
4	Lo, Chl, Pico, Cyano	0.647
6	Lo, T, Sal, Chl, Pico, Cyano	0.714
5	Lo, Sal, Chl, Pico, Cyano	0.681
5	Lo, T, Chl, Pico, Cyano	0.674
7	Lo, T, Sal, K_d, Chl, Pico, Cyano	0.734
6	La, Lo, T, Chl, Pico, Cyano	0.701
7	Lo, T, Sal Chl, PPC, Pico, Cyano	0.730
9	La, Lo, T, Sal, K_d, Chl, PPC, Pico, Cyano	0.781

Table 7. Regression output for FRRf (calculated with the Sigma and Absorption algorithms) and ^{14}C comparisons of photosynthetic parameters (P_{max}, α and E_K) for all samples, and separated into Sydney Harbour (SH) and Port Hacking (PH) samples. Reported values include the coefficient of determination (R^2) and slope of the regression ± S.E. (i.e . $\Phi_{E:C}$).

		Sigma Algorithm		Absorption Algoritm	
Parameter	**Location**	R^2	**Slope (i.e. $\Phi_{E:C}$)**	R^2	**Slope (i.e. $\Phi_{E:C}$)**
P_{max}	PH and SH	0.66	0.48 ± 0.08	0.65	1.32 ± 0.21
	SH	0.34	0.44 ± 0.16	0.34	0.34 ± 0.12
	PH	0.88	0.51 ± 0.06	0.85	1.78 ± 0.26
α	PH and SH	0.77	0.29 ± 0.04	0.59	1.95 ± 0.35
	SH	0.76	0.24 ± 0.04	0.60	0.34 ± 0.08
	PH	0.71	0.31 ± 0.06	0.67	2.36 ± 0.56
E_K	PH and SH	0.45	2.11 ± 0.52	0.45	1.14 ± 0.27
	SH	0.70	2.46 ± 0.74	0.42	1.21 ± 0.39
	PH	0.46	1.18 ± 0.28	0.58	0.81 ± 0.23

Figure 1: Sampling locations, including the Port Hacking coastal time-series station and the Sydney Harbour (Port Jackson estuary) on the east coast of Australia.

Figure 2: a) Comparison of the separate package (qP) and homogeneous method (qJ) for determining the fraction of open reaction centres; **b)** Comparison of the sigma and absorption methods for determining electron transport through PSII (Closed circles indicate SH upstream and open circles indicate PH samples) and **c)** Relative spectral output by light sources used. The *Fast*^{ACT} *MKII* source provided excitation to derive fluorescence parameters including σ_{PSII}, the photosynthetron and *Fast*^{ACT} light sources provide actinic light for the incubation of ^{14}C and fluorescence samples respectively.

Figure 3. Estimate of functional reaction centres (PSII) (mol RCII m^{-3}) in samples of varying Chl-*a* concentration from Port Hacking and Sydney Harbour. Closed circles indicate SH samples and open circles indicate PH samples. Regression line $n = 23$, $R^2 = 0.77$, $p < 0.05$.

Figure 4. Light dependency of fluorescence parameters including the **a)** functional absorption cross section (σ_{PSII}); **b)** fraction of closed reaction centres (1-qJ) and **c)** non-photochemical quenching. Closed squares and circles indicate SH upstream and downstream samples, respectively. Open squares and circles indicate PH surface and F_{max} samples, respectively.

Figure 5. The relationship between ^{14}C and FRRf derived estimates of P_{max} ($n = 19$, $R^2 = 0.66$; $p < 0.05$) **(a)**, α (α : $n = 21$, $R^2 = 0.77$; $p < 0.05$) **(b)**, and E_K (E_K : $n = 19$, $R^2 = 0.45$; $p < 0.05$) **(c).** Closed circles indicate SH samples and open circles indicate PH samples.

Figure 6. Environmental, biological and spatial variables driving divergence in the estimate of photosynthetic parameters by ^{14}C and FRRf methods. The length of the predictor variable vectors indicates the strength of their influence on the variability. **(**Lo = longitude, La = latitude, T = temperature, Sal = salinity, K_d = K_dPAR, Chl = MV Chl-*a* PPC = proportion of photoprotective pigment, Pico = picoplankton proportion, Cyano = proportion of cyanobacteria; SH = Sydney Harbour, PH = Port Hacking)

Figure 1

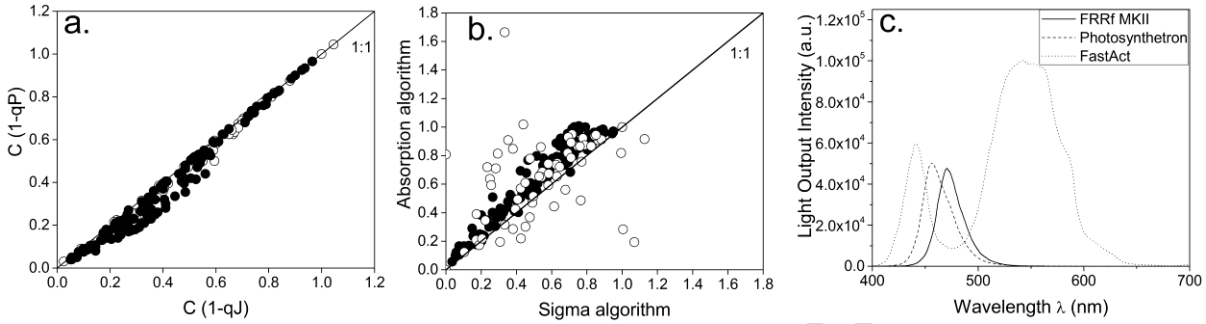

Figure 2

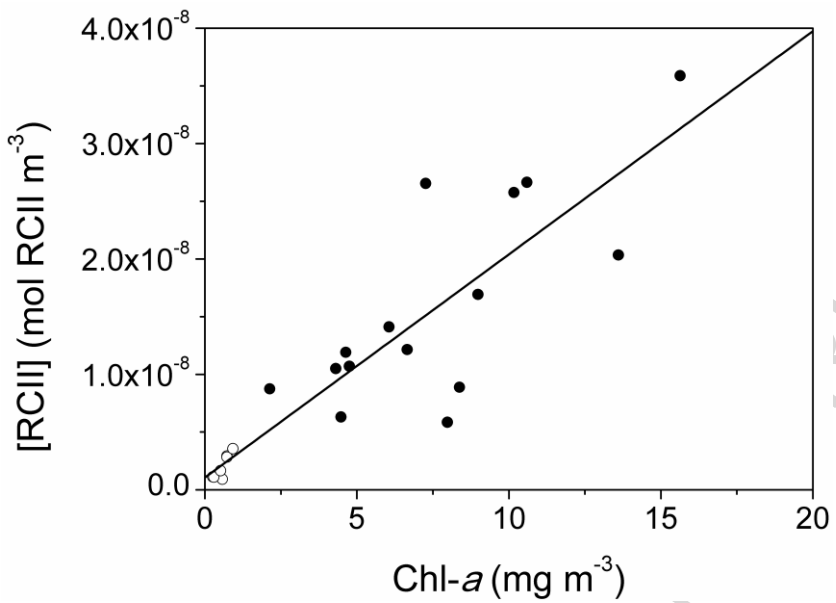

Figure 3

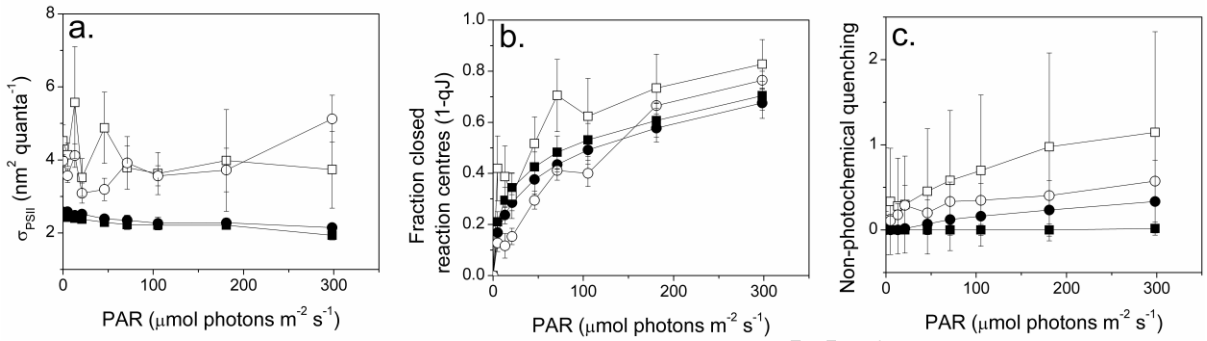

Figure 4

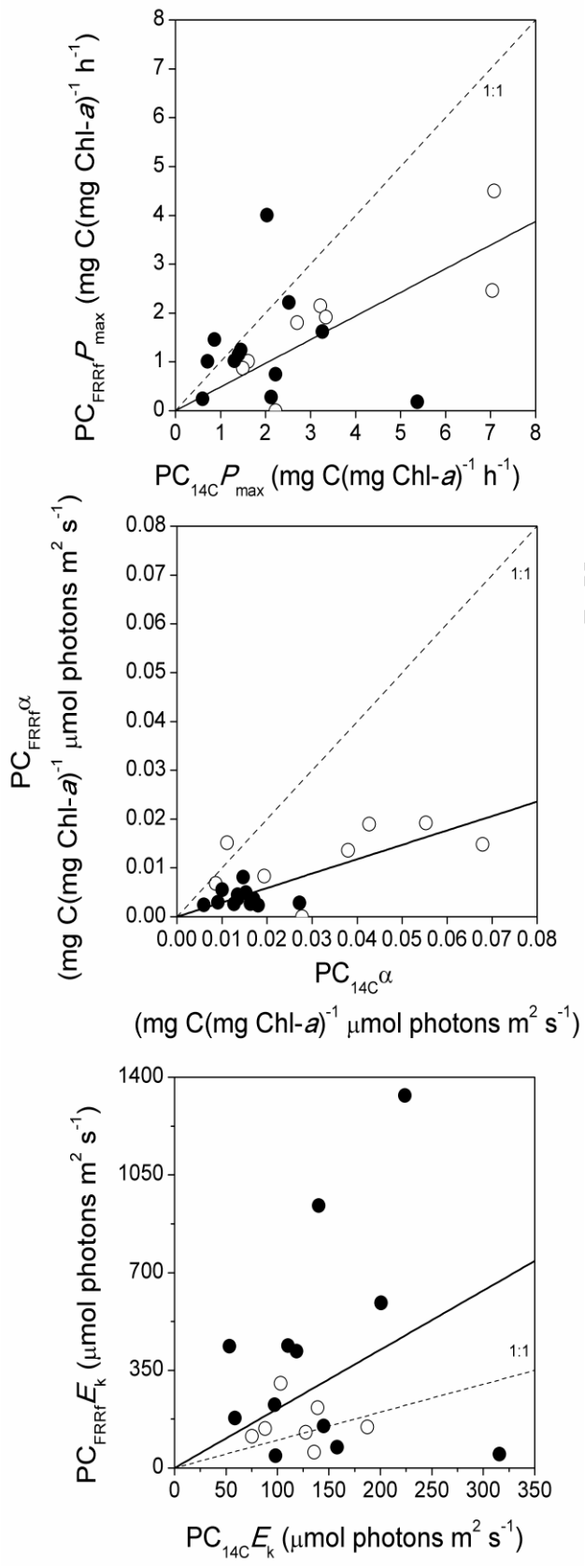

Figure 5

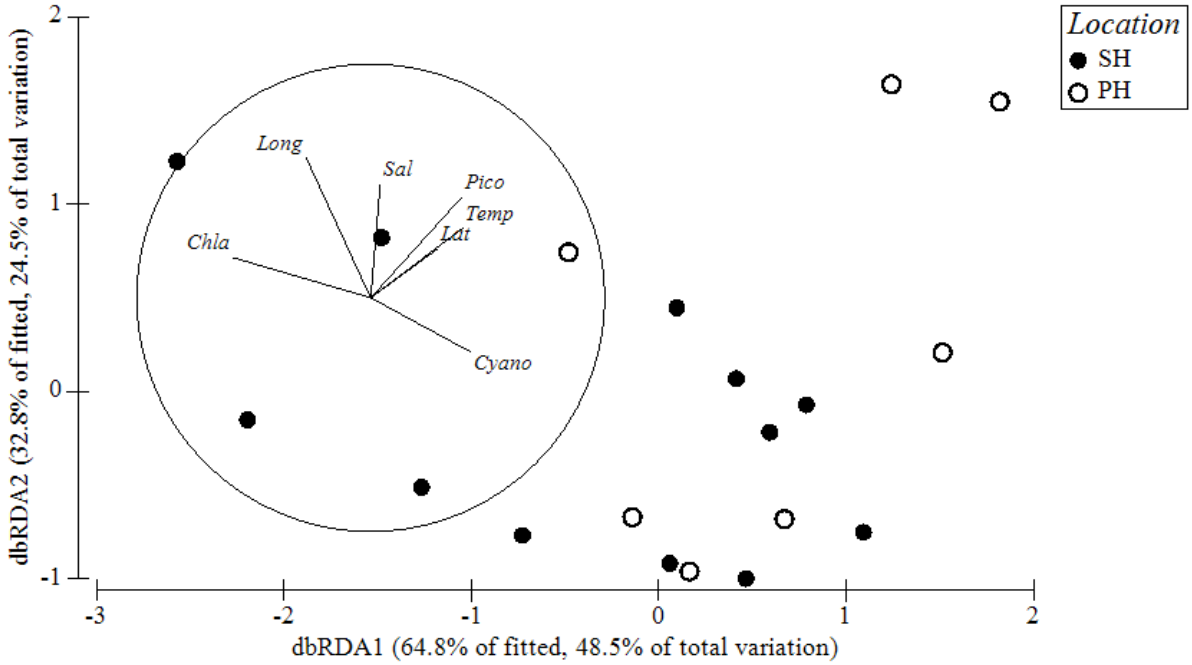

Figure 6

Highlights

- We assessed primary productivity in coastal waters using fluorometry (FRRf) and ^{14}C
- FRRf estimates of P_{max}, α and E_K were strongly correlated with ^{14}C estimates
- Primary productivity was underestimated by the Chl-a fluorescence method
- Cyanobacteria was important in driving variability between FRRf and ^{14}C estimates